The Binding of Yb(III) to Adriamycin. A ^{1}H NMR Relaxation Study

I. J. McLennan and R. E. Lenkinski*

Contribution from the Guelph-Waterloo Centre for Graduate Work in Chemistry, Guelph Campus, Guelph, Ontario, Canada N1G 2W1. *Received March 21, 1984*

Abstract: The binding of Yb(III) to adriamycin in methanol was monitored by UV-vis absorption spectroscopy. A Job ratio plot based on UV-vis binding data indicated that the complex had a stoichiometry of 1:1. The formation of the complex was found to be dependent on the hydrogen ion concentration present in methanol. The ^{1}H NMR spectrum of the Yb(III)-adriamycin complex was found to contain two sets of resonances arising from the complex and the free adriamycin indicating the rate of exchange of adriamycin between its free and complexed state was slow on the ^{1}H NMR chemical shift time scale. Transfers of magnetization experiments were carried out in order to assign the resonances arising from the paramagnetic complex. The spin-lattice relaxation times of the assigned resonances were determined. These relaxation times were analyzed in terms of the distances from the Yb(III) ion to various protons in the drug. With use of these distances and the coordinates of the hydrogen atoms obtained from an X-ray structure, the site of metal complexation was found to be at the C_{11} and C_{12} oxygens of the antibiotic characterized by an oxygen-Yb(III) bond length of 2.5 Å.

Adriamycin (Adm (I)) is an anthracycline aminoglycoside antibiotic. Adriamycin differs from daunomycin in that the CH_2OH at position 14 is replaced by CH_3. The pharmokinetic properties of Adm have been the subject of a large number of studies over the last 20 years.[3] The first reported observation of metal binding to anthracyclines was by Calendi et al. in 1965.[4] These authors found that large spectral changes occured in the visible spectrum of daunomycin upon the addition of an excess of Al(III), Fe(II), Fe(III), and Mg(II) in aqueous solution. Myers

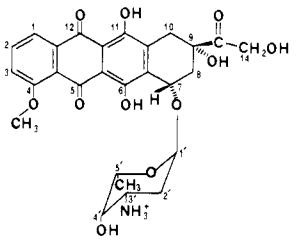

1

et al.[5] have also observed perturbations in the absorption spectrum of Adm upon binding of Fe(III) characterized by a shift from 479 to 608 nm with an isobestic point at 535 nm upon aeration in aqueous solution. From their studies the authors concluded that the species observed was probably the Fe(II)-Adm complex. Using visible absorption, CD, and ESR spectroscopy, Greenaway and Dabrowiak[6] monitored the binding of Cu(II) to daunomycin, adriamycin, and *N*-(trifluoroacetyl)daunomycin in water and have proposed that a bis Cu(II) complex of the drugs exists from pH 6.0 to 8.5. It was suggested that Adm forms a complex with Cu(II) at the quinone, hydroquinone ligands.[6] In addition, Spinelli and Dabrowiak[7] have reported the existence of a Cu(II)-daunomycin-DNA ternary complex in which the Cu(II) is bound either to the C_5, C_6 or the C_{11}, C_{12} and is not intercalated with calf thymus DNA. Fritzsche et al.[8] have suggested that iremycin, which is similar to daunomycin, forms a Cu(II) complex which also binds to DNA. However, there is very little specific geometric information concerning the metal ion binding site(s) in any of these reports. We have chosen to focus on the Yb(III) complex of Adm for a variety of reasons. We have found evidence for the existence of a ternary complex of Adm-DNA-lanthanide(III).[9] There is a large body of literature dealing with lanthanides as isomorphic replacements for Ca(II) in biological systems.[10,11] Of the paramagnetic lanthanides Yb(III) has been found to produce perturbations in the NMR spectra of ligands which are most amenable to structural interpretations (vide infra).

In a separate study using UV, visible, and fluorescence spectroscopy, we have determined the stoichiometry and the equilibrium constants for various lanthanide complexes of Adm in aqueous solution.[12] In the course of this study we found, as was previously reported by others,[13-15] that Adm undergoes self-association in aqueous solution. In the present study we present an analysis of the perturbations observed in the ^{1}H NMR spectrum of Adm induced by Yb(III). The approach used in the analysis is similar to the one employed by Sykes and co-workers in the analysis of the ^{1}H NMR spectral perturbations observed in the Yb(III)-parvalbumin complex.[16-18] As is the case with Yb(III)-parvalbumin, the rate of dissociation of the Yb(III)-Adm complex was found to be slow on the ^{1}H NMR chemical shift time scale at 400 MHz. This manifests itself in the appearance of distinct resonances of the paramagnetic complex (vide infra). These resonances were assigned by transfer of saturation techniques. The relaxation rates of these assigned resonances were analyzed in terms of the distances between the various protons and the Yb(III) center. In the following sections we present the details of these experiments as well as a geometrical model for the Yb(III)-Adm complex based on our analysis.

(1) Supported by the Natural Sciences and Engineering Research Council of Canada (R.E.L.).

(2) McLennan, I. J.; Lenkinski, R. E.; Yanuka, Y. *J. Am. Chem. Soc.*, submitted for publication.

(3) For a review see: Acamone, F. "Anticancer Antibiotics"; Academic Press: New York, 1981; Vol. 17.

(4) Calendi, E.; Di Marco, A.; Reggiani, M.; Scarpinato, B.; Valentina, L. *Biochim. Biophys. Acta* **1965**, *103*, 25-49.

(5) Myers, C. E.; Gianni, L.; Simone, C. B.; Klecker, R.; Greene, R. *Biochemistry* **1982**, *21*, 1707-1713.

(6) Greenaway, F. T.; Dabrowiak, J. C. *J. Inorg. Biochem.* **1982**, *16*, 91-107.

(7) Spinelli, M.; Dabrowiak, J. C. *Biochemistry* **1982**, *21*, 5862-5870.

(8) Fritzsche, H.; Triebel, H.; Chaires, J. B.; Dattagupta, N.; Crothers, D. M. *Biochemistry* **1982**, *21*, 3940-3946.

(9) Lenkinski, R. E., manuscript in preparation.

(10) Reuben, J. "Handbook on the Physics and Chemistry of the Rare Earths", Gschneidner, K. A., Jr., and Eyring, L., Eds.); North Holland: New York, 1979; 515-552.

(11) Reuben, J. *Naturwissenschaften* **1975**, *62*, 172-178.

(12) Lenkinski, R. E.; Sierke, S.; Vist, M. R. *J. Less.-Common Met.* **1983**, *94*, 359-365.

(13) Barthelemy-Clavey, V.; Maurigot, J.; Dimicoli, J.; Sicard, P. *FEBS Lett.* **1974**, *46*, 5-9.

(14) Martin, S. R. *Biopolymers* **1980**, *19*, 713-721.

(15) Chaires, J. B.; Dattagupta, N.; Crothers, D. M. *Biochemistry* **1982**, *21*, 3927-3932.

(16) Lee, L.; Sykes, B. D. *Biochemistry* **1981**, *20*, 1156-1162.

(17) Lee, L.; Sykes, B. D. In "Biomolecular Structure Determination by NMR" Bothner-By, A. A., Glickson, G. D., Sykes, B. D., Eds.; Marcel Dekker: New York, 1982; pp 169-188.

(18) Lee, L.; Sykes, B. D. *Biochemistry* **1983**, *22*, 4366-4373.

0002-7863/84/1506-6905$01.50/0

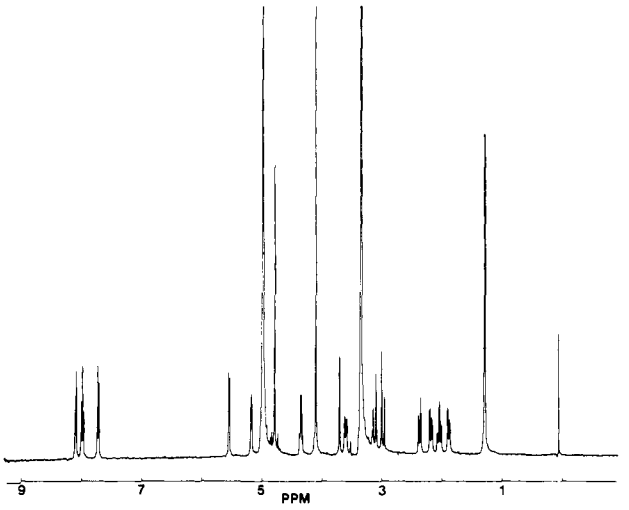

Figure 1. The 400-MHz ^1H spectrum of 4 mM adriamycin in methanol, 128 scans.

Table I. ^1H Chemical Shift Data for Adriamycin in Methanol

position	δ (ppm from DSS)	position	δ (ppm from DSS)
H1	7.97	H4′	3.66
H2	7.85	H3′	3.56
H3	7.59	H10	3.05
H1′	5.45	H8	2.36
H7	5.11	H8	2.18
H14	4.71	H2′	2.04
H5′	4.28	H2′	1.88
4-OCH_3	4.04	5′-CH_3	1.29

Materials and Methods

Adriamycin hydrochloride was kindly provided by Dr. F. Arcamone of Farmitalia Carlo Erba (Milan, Italy). The concentration of Adm was determined spectrophotometrically at a wavelength of 477 nm (ϵ = 11 500 M^{-1} cm^{-1}).[19] The solutions of Adm and Adm–Yb(III) were made up within 24 h prior to use in deuterated methanol (Merck Sharpe and Dohme). The pH of the solutions was adjusted with either 0.01 M DCl or 0.01 M NaOD (Merck). For convenience we will use the term pH to refer to the pH meter reading obtained in methanol although we realized that this does not give the hydrogen ion concentration directly. No corrections were made for deuterium isotope effects. $YbCl_3$ (99.99%) was obtained from Ventron (Danvers, MA). The concentrations of stock solutions of Yb(III) were determined by titration with EDTA with arsenazo as an indicator. The UV–vis and NMR experiments were performed at 22 ± 1 °C. The UV–vis absorption spectroscopy was performed on a Perkin Elmer Lamda 3 spectrophotometer.

The ^1H NMR experiments were performed on a Bruker WH-400 spectrometer operating at 400.13 MHz in the Fourier transform mode with quadrature detection. All ^1H NMR spectra were referenced to internal DSS (sodium (trimethylsilyl)propanesulfonate). For the transfer of magnetization experiments the decoupler power was adjusted so that one of the three aromatic protons of Adm was completely saturated but no visible perturbation in the intensities of the other peaks in the NMR spectrum was observed (on the spectrometer being used in these studies, the power level was ca 17 dB attenuation below 0.2 W). The shifted resonances of the Yb(III)–Adm complex were selectively saturated by using gated homonuclear decoupling with a decoupling time of 1 s.

The ^1H spin–lattice relaxation times were determined by the inversion recovery method (180°–τ–90°)[20] in which there were at least 10 τ values and a recycle time of 5 × T_1. The data were subsequently fit to a three-parameter exponential relationship based on a plot of the peak intensity vs. τ.

Results and Discussion

Figure 1 shows a ^1H NMR spectrum of 5 mM Adm in deuterated methanol at 400 MHz. Since Adm self-associates in water, the present study was performed in methanol where we have found no evidence for self-association.[2] The peak assignments are presented in Table I. Upon the addition of 2.5 mM $YbCl_3$ a new set of peaks is seen at lower frequency (Figure 2). It can be seen by a comparison of Figure 2 with Figure 1 that the resonance positions of the peaks in the original diamagnetic spectrum of Adm are not altered. Thus we can conclude that the paramagnetic Yb(III)–Adm complex is in slow exchange on the ^1H NMR time scale with free Adm under these conditions. It is likely that the Yb(III)–Adm complex in methanol still may have chlorines in some of the coordination sites. However, this will not affect any of the geometrical conclusions reached regarding the site of complexation of Yb(III) on Adm. With Yb(III) in particular, the paramagnetic interactions can give rise to large shifts which are dipolar in origin with minimal broadening of the shifted resonances. This is seen in Figure 2, and therefore the set of peaks at lower frequency are resonances arising from the paramagnetic complex (Yb(III)–Adm). Analogous experiments were performed with La(III) in order to determine the magnitude of the diamagnetic contribution to the overall shift. Upon the addition of La(III) there was found to be little (<5 Hz) or no shift of the resonances in the spectrum of Adm. Therefore, the diamagnetic contribution to the shifts seen in Figure 2 is negligible. Attempts

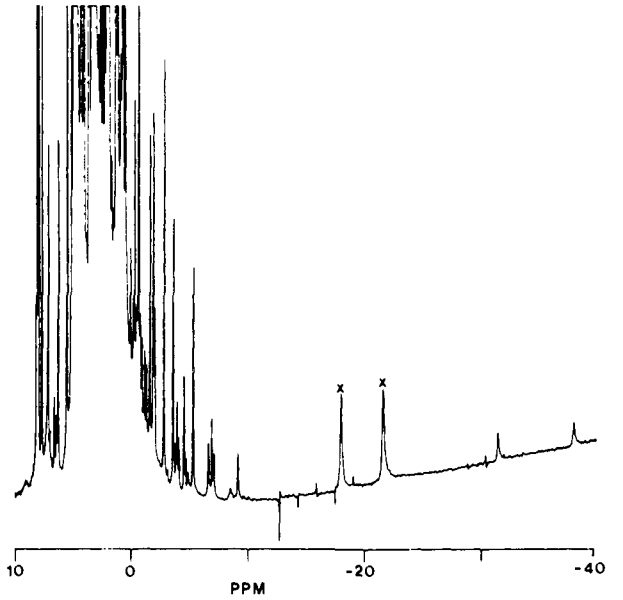

Figure 2. The 400-MHz ^1H spectrum of 5 mM Adriamycin + 2.5 mM $YbCl_3$ in methanol, 500 scans, sweep width 40 000 Hz. The two peaks marked with an X do not arise from the Yb(III)–Adm complex. In comparison to the other peaks at −32 and −39 ppm the aforementioned peaks arise from more than one proton.

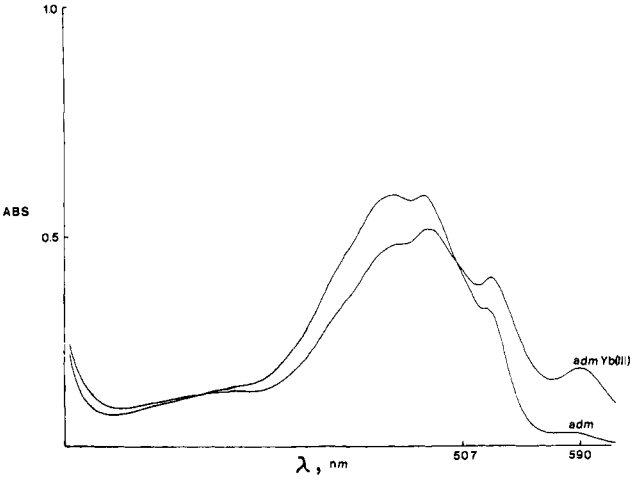

Figure 3. UV–vis absorption spectrum of adriamycin in methanol 5.3 × 10^{-5} M Adm, and with the addition of 1 × 10^{-5} M $YbCl_3$.

(19) Gabbay, E. J.; Grier, D.; Fingerle, R. E.; Reiner, R.; Levy, R.; Pearce, S. W.; Wilson, W. D. *Biochemistry* **1976**, *15*, 2062–2070.
(20) Vold, R. L.; Waugh, J. S.; Klein, M. P.; Phelps, D. E. *J. Chem. Phys.* **1968**, *48*, 3831–3832.

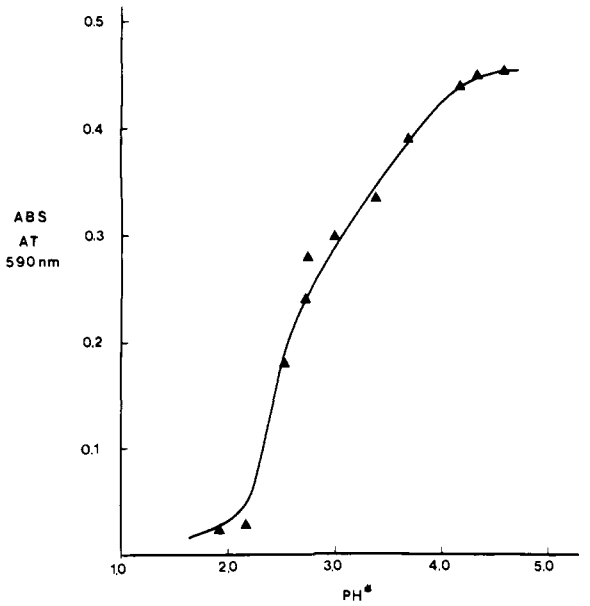

Figure 4. The pH dependence of Yb(III) binding to adriamycin in methanol. The absorbance of the peak at 590 nm was monitored. The line is an empirical fit to the data.

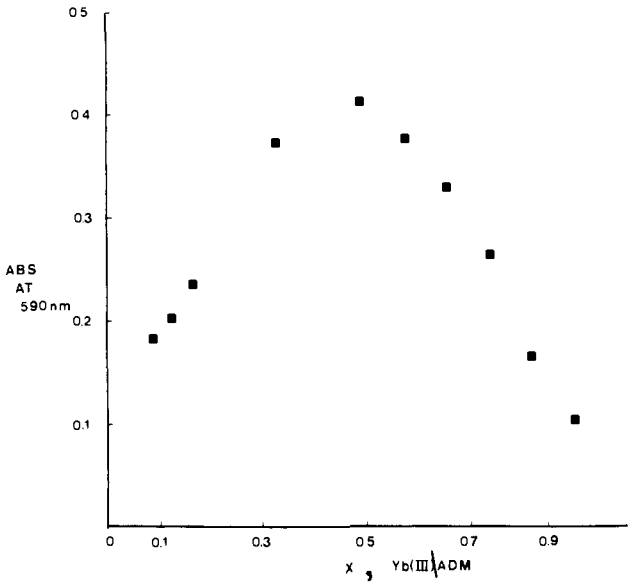

Figure 5. A Job ratio plot of Yb(III) binding to adriamycin in methanol. The symbol X refer to the mole fraction of the Yb(III)–Adm complex.

were made to observe the Yb(III)–Adm complex in water; however, the ^{1}H NMR spectrum of the complex was severely broadened.

Upon addition of $YbCl_3$ to a solution of Adm in methanol we also observed large perturbations in the UV–vis absorption spectrum. Specifically, there is a shift in λ_{max} from 480 to 590 nm with an isosbestic point at 509 nm. This can be seen from the spectra shown in Figure 3. A similar change in the UV–vis absorption spectrum of Adm upon Ln(III) binding has also been observed in water.[9] The pH dependence of Yb(III) binding to Adm in methanol is shown in Figure 4. These data were obtained by monitoring the appearance of the peak at 590 nm which arises from the Yb(III)–Adm complex. We made no attempt to analyze these data rigorously. We did, however, use these results to provide an estimate of the extent of complex formation. Thus at a pH of 2.9 ± 0.6 we estimate that half of the Yb(III) is complexed. For the stoichiometry of the Yb(III)–Adm complex to be determined, a Job ratio plot[21] was constructed by using the absorbance at 590 nm to monitor complex formation (Figure 5). The Job plot indicates the formation of a 1:1 complex of Yb(III) with Adm in methanol.

(21) Job, P. *Ann. Chem.* **1936**, *6* (11), 99–144.

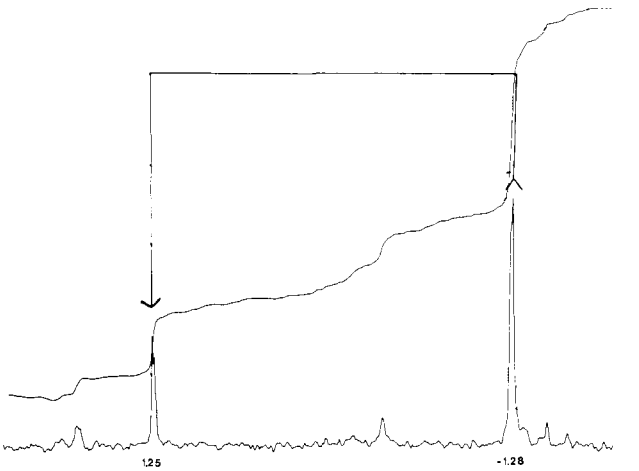

Figure 6. A transfer saturation experiment in which the peak at −1.28 ppm was irradiated for 1 s. The difference spectrum shown is the subtraction of the control spectrum from the irradiated spectrum. Each spectrum was the sum of 500 scans. The concentration of adriamycin was 4 mM, $YbCl_3$ 2.1 mM, pD in methanol was 4.2, T = 22 °C.

The assignment of a number of nuclei near the Yb(III) binding site in Adm was accomplished by NMR transfer of saturation experiments. Transfer of saturation is governed by the equation

$$(M_0^\alpha - M_z^\alpha)/M_0^\alpha = [T_{1\alpha}/(T_{1\alpha} + \tau_\alpha)][(M_0^\beta - M_z^\beta)/M_0^\beta] \quad (1)$$

based on the derivation by Gupta and Redfield.[22] The superscripts α and β refer to the two nuclei which are chemically exchanging. $T_{1\alpha}$, τ_α, M_z^α and M_0^α are the spin–lattice relaxation time, lifetime, observed magnetization, and equilibrium magnetization of the α nucleus, respectively. The analogous notation is used for the β nucleus. The term $(M_0^\alpha - M_z^\alpha)/M_0^\alpha$ represents the fractional decrease in the intensity of the α resonance resulting from the irradiation of the β resonance. The extent (η) of transfer of saturation, η, is dependent on the lifetime of the paramagnetic complex that gives rise to the dipolar shifts and to the spin–lattice relaxation time of the complex, i.e.,

$$\eta = \frac{T_{1M}}{T_{1M} + \tau_M} \quad (2)$$

where T_{1M} and τ_M are the spin–lattice relaxation time and lifetime of the complex, respectively. Figure 6 shows the extent of transfer of saturation from a resonance at −1.28, ppm to the resonance at 1.25 ppm which has been assigned to the 5′-methyl group. Therefore the peak at −1.28 ppm arises from the 5′-methyl in the Yb(III) complex. In a similar way, resonances from the shifted peaks in the region −39 ppm to −2 ppm were assigned. Using eq 2, the value of η, the extent of transfer of saturation, and the value of T_{1M} of the particular resonance in the complex, we can determine τ_M, the lifetime of the Yb(III)–Adm complex. This calculation was carried out for the 5′-methyl shown in Figure 6, where η was found to be 33%. In a separate experiment we determined T_{1M} to be 0.392 s for this resonance. Using these results in eq 2 we calculated the lifetime for the Yb(III)–Adm complex of 0.81 s.

The binding of paramagnetic metals such as Yb(III) usually leads to enhancements of the relaxation rates of nearby nuclei.[23] These perturbations can be used to calculate absolute distances from the paramagnetic metal to the nucleus.[24] The spin–lattice

(22) Gupta, R. K.; Redfield, A. G. *Biochem. Biophys. Res. Commun.* **1970**, *41*, 273–281.

(23) Reuben, J.; Elgavish, G. A. "Handbook of the Physics and Chemistry of Rare Earths", Gschneider, K. A., Jr., Eyring, L., Eds.; North Holland: New York, 1979.

Table II. Summary of Distances from the Yb(III) Binding Site Calculated from T_1 Measurements and from the Molecular Model

nucleus	δ	T_1, s	R,[a] Å	R,[b] Å	R,[c] Å
H10	−39	0.0144	4.13	4.05	7.75
H10	−32	0.0205	4.38	4.63	7.08
H8	−9.4	0.133	5.98	6.05	5.80
H7	−7.2	0.206	6.44	6.73	5.30
H8	−5.6	0.142	6.05	7.13	6.50
H2′	−4.9	0.122	5.90		

[a] Calculated from T_1 measurements. [b] Calculated from the model with Yb(III) binding to C_{11}, C_{12}. [c] Calculated from the model with Yb(III) binding to C_5, C_6.

relaxation time of nuclei in the presence of a paramagnetic lanthanide (non-S states) is dominated by dipolar relaxation.[23] The equation describing these perturbations contains two terms, the conventional dipolar term and a susceptibility term recently derived by Vega and Fiat[25] and Gueron.[26] The conventional dipolar term can be expressed as

$$\frac{1}{T_{1M}} = \frac{2}{15}\frac{\gamma_I^2 g^2 J(J+1)\beta^2}{r^6}\left(\frac{3\tau_c}{1+\omega_I^2\tau_c^2} + \frac{7\tau_c}{1+\omega_s^2\tau_c^2}\right) \quad (3)$$

where T_{1M} is the spin–lattice relaxation time of the particular nucleus in the lanthanide metal complex, γ_I is the nuclear magnetogyric ratio, g is the Landē g factor, β is the Bohr magneton, r is the vector distance between the paramagnetic lanthanide and the nucleus being monitored, ω_I is the nuclear larmor frequency, $\omega_s \approx 660\omega_I$, and τ_c is given by

$$\frac{1}{\tau_c} = \frac{1}{\tau_R} + \frac{1}{T_{1e}} + \frac{1}{\tau_M} \quad (4)$$

where τ_R is the rotational correlation time of the complex, T_{1e} is the electron spin relaxation time, and τ_M is the lifetime of the lanthanide ligand complex. From eq 3 it is clear that there is a very strong dependence between the spin–lattice relaxation time and distance, r. The other contribution to the spin–lattice relaxation time is the susceptibility term, and it is described as follows[25,26]

$$\frac{1}{T_{1M_\chi}} + \frac{6}{5}\frac{\gamma_I^2 H_0^2 g^4 \beta^4 J^2 (J+1)^2}{(3kT)^2 r^6}\left(\frac{\tau_R}{1+\omega_I^2\tau_R^2}\right) \quad (5)$$

where T_{1M_χ} is the spin–lattice relaxation arising from the magnetic susceptibility, T is the temperature, k is the Boltzman constant, and all the other terms have been defined previously. The relative importance of these two contributions to the spin–lattice relaxation rates in the Yb(III) complex can be determined by dividing eq 5 by eq 3 to give the following relationship

$$(1/T_{1_\chi})/(1/T_{1S}) = \frac{9}{10}\frac{g_L^2\beta^2 J(J+1)H_0^2}{(3kT)^2}\frac{1}{T_{1e}}\left(\frac{\tau_R}{1+\omega_I\tau_R^2}\right) \quad (6)$$

where the subscript S refers to the Solomon term[28] and χ refers to the susceptibility term. With use of a value for τ_R of 6×10^{-11} s (determined from ^{2}H relaxation time measurements) and a T_{1e} of 2.2×10^{-13} s,[27,29] with $H_0 = 9.42$ T for Yb(III), the ratio $(1/T_{1_\chi})/(1/T_{1S})$ is equal to 7×10^{-4}. Therefore the conventional dipolar term can be used to describe the spin–lattice relaxation time of the Yb(III) complex, and the electron spin–lattice relaxation time is the dominant correlation time in eq 3. Equation 3 can be rewritten in terms of the electron spin relaxation time

$$\frac{1}{T_1} = \frac{T_{1e}}{r^6}C \quad (7)$$

where $C = 1.73 \times 10^{-30}$ cm^6 s^{-2}. For Yb(III), $T_{1e} = 2.2 \times 10^{-13}$ s[27,29] and eq 7 can be solved in terms of r as

$$r = \sqrt[6]{2.36 \times 10^{-43} T_{1M}} \quad (8)$$

The distances between seven ^{1}H nuclei and the Yb(III) ion were calculated by using eq 8. Table II summarizes the T_1 data and distances for these particular nuclei. A scale model of the Yb(III)–Adm complex was constructed based on the known crystal coordinates of daunomycin which is similar to Adm.[30]

The distances derived from our value of the T_1 data were fit to the model by using an iterative procedure in order to determine the site of metal binding in Adm. The best fit was found to be with the metal coordinated to the quinone, hydroquinone on the C_{12}, C_{11} oxygens in the plane of the ring system (Figure 7). The computational procedure involved generating the orthogonal coordinates from the X-ray data[30] and solving the distance formula $r = ((a - x_i)^2 + (b - y_i)^2 + (c - z_i)^2)^{1/2}$ where r is the distance from the metal to the particular nucleus, a, b, and c are the coordinates of the metal ion, and x_i, y_i, and z_i are the coordinates of the nuclei derived from the X-ray data. The values of a, b, and c were varied until the best fit was obtained to the T_1 data. However, when attempts were made to fit the distances to the proposed binding site in the model, the distance did not fit to the conformation of the A ring which has a 30° pucker in the crystal. The conformation of the A ring was reexamined, and it was determined that the best fit to the T_1 data was found to be when the A ring had a 40° pucker. In Table II it is seen that there is good agreement between the distances based on the T_1 data and the calculated data on the A ring having the 40° pucker. It should be noted that in the "altered" conformation there is little steric strain imposed upon the molecule. For comparison we have also included in Table II the calculated distances using the model with the Yb(III) atom at the C_5, C_6 site. As can be seen from the data there is a large discrepancy in the distances in comparison to the C_{11}, C_{12} site.

We should point out that in the above analysis of the distances we have assumed only one conformation of Adm. In order to avoid using resonances where conformational averaging is likely to occur, we used only perturbations observed in the resonances in the ring system of the antibiotic in our analysis. Distances were calculated for several nuclei on the sugar moiety. One of these, the 2′-hydrogen, is reported in Table II. On the basis of this distance, the sugar ring in the molecular model is positioned such that it is in a similar conformation to that reported by Nokata and Hopfinger[31] based on conformational energy maps for the two torsional rotational angles in the glycosidic linkage between the C_7 on the

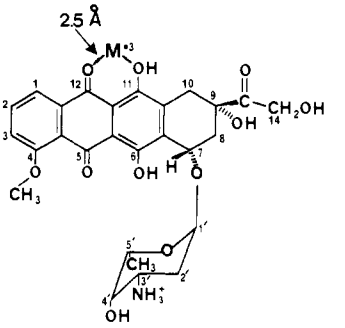

Figure 7. The binding site for Yb(III) in adriamycin in methanol on the basis of the analysis of the relaxation rates of the protons shown in Table II.

(24) Bleaney, B. *J. Magn. Reson.* **1972**, *8*, 91–100.
(25) Vega, A. J.; Flat, D. *Mol. Phys.* **1976**, *31*, 347–355.
(26) Gueron, M. *J. Magn. Reson.* **1975**, *19*, 58–66.
(27) Reuben, J.; Flat, D. *J. Chem. Phys.* **1969**, *51*, 4918–4927.
(28) Solomon, I. *Phys. Rev.* **1955**, *99*, 559–565.
(29) Lenkinski, R. E.; Reuben, J. *J. Magn. Reson.* **1976**, *21*, 47–56.
(30) Courseille, C.; Dusetta, B.; Geoffre, S.; Hospital, M. *Acta Crystallogr., Sect. B* **1979**, *B35*, 764–767.
(31) Nakata, Y.; Hopfinger, A. J. *FEBS Lett.* **1980**, *117*, 259–264.

A ring and the C1 of the sugar.

Conclusions

We have established that Yb(III) binds to a unique position on the C_{11}, C_{12} oxygens in the plane of the ring system of Adm. The possibility that the Yb(III) ion binds to the other quinone, semiquinone system (C_5, C_6 oxygens) can be excluded on the basis of the distances determined from the T_1 data, i.e., there is only one reasonable fit to the T_1 data. This is the model in which the Yb(III) resides at the C_{11}, C_{12} binding site in Adm. The results of this study illustrate the potential utility of analyzing Yb(III)-induced relaxation rate enhancements in terms of internuclear distances. We are currently extending the analysis of this paper to determine the conformation of the sugar ring of Adm in methanol.

Acknowledgment. The NMR experiments were performed at the South Western Ontario NMR Centre at Guelph funded by a major installation grant from the Natural Sciences and Engineering Research Council of Canada.

Behavior of Hexane Dissolved in Dioleoylphosphatidylcholine Bilayers: An NMR and Calorimetric Study†

Russell E. Jacobs* and Stephen H. White

Contribution from the Department of Physiology and Biophysics, University of California, Irvine, California 92717. *Received April 18, 1984*

Abstract: Deuterium nuclear magnetic resonance (NMR) spectroscopy and differential scanning calorimetry (DSC) have been used to examine the behavior of 1,2-dioleoyl-*sn*-glycero-3-phosphatidylcholine (DOPC) bilayers to which hexane has been added. This work represents an extension of an earlier study of hexane dissolved in dimyristoylphosphatidylcholine (DMPC) bilayers. Both differences and similarities in the two bilayers are oberved. DSC thermograms indicate that hexane incorporated into DOPC bilayers behaves as a simple impurity—the lipid phase transition is broadened and shifted to lower temperatures by the addition of hexane. Deuterium NMR spectra of perdeuterated hexane in the bilayers show three overlapping powder patterns, indicating that on average both ends of the molecule are experiencing the same environment. The temperature dependence of the hexane deuterium quadrupole splittings exhibits a maximum at the lipid bilayer phase transition temperature. The hexane powder patterns coalesce into a single line under conditions of low temperature and high concentration, indicating the onset of isotropic motion. Deuterium NMR spectra of 1,2-(9′,10′-$^2H_2$)DOPC consist of four overlapping powder patterns which change little upon the addition of up to 50 mol % hexane. Thus, the bilayer stays intact and the motional characteristics of the DOPC double bonds are not changed by the presence of even an equimolar mixture of the alkane.

The lipid bilayer constitutes the principal structural features of the biological membrane.[1] A variety of hydrophobic components exist naturally within the bilayer (e.g., membrane proteins and cholesterol)[2,3] or can be introduced artificially (e.g., general anesthetics).[4,5] The lipid bilayer is essentially a "solvent" for hydrophobic "solute" molecules. A quantitative understanding of the solvent properties of lipid bilayers is essential for understanding membrane structure, the insertion and translocation of proteins into and across membranes, and the mechanisms of membrane active drugs. In order to characterize the interactions between bilayer lipid and hydrophobic components in detail, we are examining simple model systems. In the work reported here, hexane is employed as a prototypal hydrophobic molecule and the bilayer is constructed from a single type of lipid. In a previous study, we examined the hexane/DMPC bilayer system.[6] We found that the alkane behaves in a very nonideal manner and that an unusually large amount of hexane could be incorporated into the bilayer without affecting the motional behavior of the lipids.

We present here information about the behavior of the hexane/DOPC bilayer system. Differential scanning calorimetry thermograms indicate that hexane acts as a simple impurity—even at concentrations in the bilayer equimolar with the lipid. ^2H NMR powder patterns give direct information about the average order imposed upon the alkane by the bilayer and, by inference, information about the types of anisotropic motion being executed by the labeled molecule.[7,8] The ^2H NMR spectra of bilayers of DOPC labeled at the double bonds are essentially unaffected by the addition of hexane. The spectra consist of four overlapping powder patterns, one from each of the four deuterons. ^2H NMR spectra of perdeuterated hexane dissolved in DOPC bilayers reveal that the types of motion that this small molecule undergoes in the bilayer are strong functions of both temperature and concentration.

Experimental Procedure

^2H labeled and unlabeled DOPC were purchased from Avanti Polar-Lipids, Inc. (Birmingham, AL), deuterium-depleted water (^2H content = 1% of natural abundance) from Sigma (St. Louis, MO), hexane (pesticide grade) from Burdick and Jackson Laboratories, Inc. (Muskegon, MI), perdeuterated hexane from KOR Isotopes, Inc. (Cambridge, MA), and ^{14}C-labeled DOPC was from New England Nuclear (Cambridge, MA). Tritiated hexane was synthesized from 1-bromohexane via reduction with $LiAl^3H_4$ and $LiAl^2H_4$. All alkanes used were checked for purity by using gas chromatography and found to be greater than 99% pure. Thin-layer chromatography was used to monitor lipid purity.

A series of mixtures of DOPC, hexane, and ^2H-depleted water were prepared. Samples were prepared in essentially the same manner as

† This work was supported by grants from the National Science Foundtion (PCM-8104581) and National Institutues of Health (GM-26346).

(1) Singer, S. J.; Nicolson, G. L. *Science (Washington, D.C.)* **1972**, *175*, 720-731.
(2) Silvius, J. R. In "Lipid-Peptide Interactions"; Jost, P. C., Griffiths, O. H., Eds.; Wiley: New York, 1982; Vol. 2, Chapter 7.
(3) Lentz, B. R.; Barrow, D. A.; Hoechli, M. *Biochemistry* **1980**, *19*, 1943-1954.
(4) Hill, M. W. "Molecular Mechanisms in General Anesthesia"; Halsey, M. J., Miller, R. A., Sutton, J. A., Eds.; Churchill-Livingstone: Edinburg, England, 1974.
(5) Mullins, L. J. "Molecular Mechanisms of Anesthesia"; Fink, B. R. Ed.; Raven Press: New York, 1975; Vol. 1, p 237.
(6) Jacobs, R. E.; White, S. H. *J. Am. Chem. Soc.* **1984**, *106*, 915-920.
(7) Jacobs, R.; Oldfield, *Prog. Nucl. Magn. Reson. Spectrosc.* **1980**, *14*, 113-136.
(8) Seelig, J. *Q. Rev. Biophys.* **1977**, *10*, 353.

0002-7863/84/1506-6909$01.50/0